Journal of Research in Pharmacy

Research Article

www.jrespharm.com

Application of Box-Behnken design in the optimization of chitosan nanoparticles prepared by the ionic gelation-ultrasonication method and evaluation of dispersion stability

Setenay ÖZER-ÖNDER [1,2], Timuçin UĞURLU [1 *]

1 Department of Pharmaceutical Technology, Faculty of Pharmacy, Marmara University, Maltepe 34854 İstanbul, Türkiye.
2 Institute of Health Sciences, Marmara University, Kartal 34865, İstanbul, Türkiye.
* Corresponding Author. E-mail: tugurlu@marmara.edu.tr (T.U.); Tel. +90-0216-777-52-00-5451.

Received: 12 February 2024/ Revised: 11 March 2024 / Accepted: 11 March 2024

ABSTRACT: The main objective of this study was to optimize chitosan nanoparticles by exploring the relationship between design factors and experimental data through response surface methodology. A Box-Behnken design was employed, considering chitosan: tripolyphosphate ratio (X_1), pH of the chitosan solution (X_2), and ultrasonication amplitude (X_3) as independent factors. Particle size, polydispersity index (PDI), and zeta potential served as the dependent variables. Nanoparticles were successfully prepared using a modified ionic gelation method incorporating an ultrasonic homogenizer and evaluated by models according to Box-Behnken Design. Surface plots were utilized to enhance the understanding of interactions between different variables. Results indicated that the chitosan ratio played the most significant role on both particle size and polydispersity, while the ultrasonic homogenizer amplitude predominantly influenced zeta potential. The models for particle size and polydispersity exhibited high accuracy (R^2, 0.9992 and 0.9955, respectively), whereas the zeta potential model demonstrated a lower R^2 value (0.7857) and lack of statistical significance. Comparison of predicted and actual data revealed larger error% values in the zeta potential model, exceeding the acceptable 15% threshold. Consequently, it was concluded that the ionic gelation-ultrasonic homogenizer technique, coupled with the Box-Behnken Design, is a rapid and effective approach for chitosan nanoparticle preparation and optimization. Additionally, aqueous dispersions of nanoparticles exhibited significant changes in particle size, polydispersity, and zeta potential values over one month at temperature and relative humidity conditions in accordance with ICH stability guidelines. This reinforced the recommendation that nanoparticles should be lyophilized and stored in a dry form.

KEYWORDS: Chitosan; nanoparticle; Box-Behnken design; DoE; stability.

1. INTRODUCTION

Nanotechnology, which includes all the technological developments functioning at the nanometer scale, has permeated diverse scientific disciplines in last decades such as medicine, engineering, electronics, and so on. This multidisciplinary influence underscores its significance as one of the most promising technological advancements of the 21st century [1]. Among all these applications, drug delivery stands out as one of the most promising fields, wherein nanoparticles serve as carriers releasing their cargo in a controlled manner, protecting drug against the environment, and facilitating the targeted delivery of therapeutic agents to specific cells or tissues within the physiological milieu. The enhanced pharmacokinetic properties attributed to nanoparticles stem from their distinctive physical nature and reduced dimensions. Their diminished size enables a larger surface area, and also a targeting ability of specific cells, thereby allowing for selective actions contingent upon the specific characteristics of the nanoparticle [2, 3].

The utilization of polymeric nanoparticles represents an efficacious strategy for the drug delivery, given their inherent amenability and morphology which can be modified according to specific requirements. Various types of polymers, including alginic acid, gelatin, polylactic acid, chitosan, polylactide-co-glycolide, and polycaprolactone, are commonly employed in the construction of these nanocarriers [4]. Chitosan (CS), a natural polymer derived from chitin, has gained significant attention in the field of nanotechnology. Its appeal lies in its attributes of biodegradability, biocompatibility, and non-toxicity, rendering it a versatile

How to cite this article: Özer-Önder S, Uğurlu T. Application of Box-Behnken design in the optimization of chitosan nanoparticles prepared by the ionic gelation-ultrasonication method and evaluation of dispersion stability. J Res Pharm. 2024; 28(4): 1057-1068.

ISSN: 2630-6344

http://dx.doi.org/10.29228/jrp.788

material suitable for deployment as a drug carrier across diverse applications [5, 6]. The mucoadhesive properties of CS contribute to prolonged residence time in the application site, enhancing absorption and subsequent bioavailability [7]. Its inherent cationic charge establishes a pronounced affinity for nucleic acids, positioning CS as an efficacious carrier for genetic materials and proteins [8, 9]. Furthermore, the amino group within CS demonstrates an inhibitory effect on bacterial growth by binding to surface components, thus showing antibacterial activity [10]. Beyond these characteristics, CS exhibits noteworthy potential in vaccine research, owing to its immune-stimulating properties [11, 12].

The size, polydispersity index (PDI), and surface charge of nanoparticles play crucial roles in determining their passive targeting ability, distribution, cellular uptake, membrane interactions, absorption, and in vivo stability [13]. Therefore, these three parameters appear as critical process parameters (CCP) in nanoparticle optimization. In this case, employing statistical methods can reduce the necessity for extensive preformulation studies, leading to time and material savings. Within this statistical approach, design of experiments (DoE) can be used to establish correlations between independent variables (CCP) and dependent variables (responses) in formulation step of nanoparticles and determine significant and insignificant factors for the desired responses. Thus, DoE allows optimization of formulation parameters with limited runs based on a statistical method [14]. Response Surface Methodology (RSM) is a DoE method that encompasses a set of valuable statistical techniques used to analyze the effects of multiple independent variables [15]. There are different methods within RSM such as central composite design and Box-Behnken. Box-Behnken Design (BBD) is a RSM in which at least three factors can be examined at three levels: low, medium and high. Unlike the central composite design, which requires up to twenty runs and five factor levels, BBD requires fewer runs, including three center points and three variable levels while excluding runs at the extreme levels. It is therefore more cost-effective than central composite designs with the same number of factors [16, 17].

In this study, we examined the effects of independent variables and their interactions on the properties of CS nanoparticles using BBD to determine the optimal conditions to produce the desired formulation. Further, the impact of simultaneous incorporation of an ultrasonic homogenizer to the ionic gelation technique investigated and 17 independent experiments suitable for BBD were run for this aim. Particle size, particle charge (zeta potential), and PDI were then measured for each formulation, and the average data were entered into the Design Expert software, enabling the construction of a comprehensive model for further analysis and interpretation. After the DoE analysis, stability studies were also carried out by monitoring particle size, PDI and zeta potential under different temperature and humidity conditions in order to interpret the physical stability of dispersions of different formulations.

2. RESULTS AND DISCUSSION

2.1. Statistical analysis

2.1.1. Effects on particle size

Particle size affects many properties in drug delivery systems, such as dissolution and release rate, bioavailability, in vivo distribution, targeting and deposition properties. Hence, it is a critical parameter in formulation optimization. In this study, the particle size of different formulations (Y_1) was analyzed through multiple regression using three independent variables (X_1, X_2, and X_3), as outlined in the presented DoE model. This analysis aimed to establish a regression equation that could effectively reflect the relationship between the response and the experimental data. In the design for particle size response, the equation that provides a high R^2 value to ensure the accuracy of the study was the cubic model (Table 1). The equation is found as:

$$Y_1 = 208.01 + 282.82\,X_1 - 107.48\,X_2 - 187.09\,X_3 - 12.58\,X_1X_2 - 175.14\,X_1X_3 + 129.53\,X_2X_3 + 52.81\,X_1^2 - 59.41\,X_2^2 + 165.64\,X_3^2 + 99.66\,X_1^2X_2 - 26.43\,X_1X_3^2 - 205.23\,X_1X_2^2 \quad (1)$$

The positive coefficient preceding a factor in the regression equation signifies that the response increases with the factor, while a negative coefficient implies the converse effect [18]. According to this equation, as the chitosan ratio (X_1) increased from 3 to 7 in the formulation, the particle size simultaneously increased. On the contrary, as the pH value (X_2; from 4,2 to 5,0) and the amplitude of the ultrasonic homogenizer (X_3; from 0 to 80%) increased, the particles became smaller (Figure 1-a,b). The measured particle size varied from 105.1 to 1097.93 for various factor-level combinations (Table 2).

Depending on the coefficients, it was seen that the biggest effect on the particle size belonged to that of chitosan ratio. Viscosity of the polymer solution is known to vary depending on concentration and this change affects the droplet size which also influences the particle size conversely [19]. Different studies support that particle size increases with increasing chitosan concentration [20].

The effect on particle size was represented as a cubic equation model, where each factor also affected the average size value interactively with other factors. In addition to the individual or binary effects of the independent variables in the model, some of the cubic coefficients also had a significant effect on particle size with a *p* value less than 0.01 as seen in ANOVA results (Table 1). Moreover, the model F-value of 424.58 implies the model is significant at the 5% level.

The 3D surface graph in Figure 1-a, illustrates the change in particle size values based on three independent variables. Given that it is a third-order model, this graph clearly implies a complex relationship between all three factors, collectively influencing the final particle size value.

2.1.2. Effects on polidispersity index

As a measure of particle size uniformity, the effect of independent variables on particle size distribution was considered by measuring PDI (Y_2). In the study, the model that most accurately explained the effect of independent variables on polydispersity was the cubic equation with a coefficient of determination of 0.9955 and a *p* value less than 0.001. ANOVA results of the cubic mathematical model for PDI is given in Table 1. Also, the model F-value of 73.59 implies the model is significant at the 95%. The regression equation is given below.

$$Y_2= 0.526+ 0.202\ X_1- 0.162\ X_2- 0.056\ X_3+ 0.044\ X_1 X_2- 0.029\ X_1 X_3- 0.003\ X_2 X_3- 0.064\ X_1^2- 0.046\ X_2^2+ 0.133\ X_3^2+ 0.155\ X_1^2 X_2- 0.058\ X_1^2 X_3- 0.166\ X_1 X_2^2 \quad (2)$$

Since having the highest value among all coefficients, seen that the CS ratio affected the particle polydispersity linearly and most strongly compared to that of other factors. In addition, the particle size distribution became more uniform as the chitosan pH increased from 4.2 to 5.0 or the applied ultrasonic amplitude increased from 0 to 80%.

The response surface plot and cubic design of BBD for PDI were illustrated in Figure 1-c, d. In addition to the individual effects of the factors on size uniformity, the effect of the cubic model formed due to their dual effects on the PDI was also clearly seen in the 3D plot.

2.1.3. Effects on zeta potential

The high surface area of nanoparticles causes a high surface energy. Particles that attempt to reduce high surface energy tend to agglomerate, resulting in rapid precipitation of dispersed nanoparticles, creaming, crystal growth, and variable dosing for the drug [21]. Herein, zeta potential is regarded as a key indicator and serves as a crucial factor for achieving high stability. Therefore, the zeta potential of the particle was chosen as a CPP in this study.

The regression model explaining the relationship between the independent variables and zeta potential (Y_3) of the formulations was assessed by the equation:

$$Y_3= 27.09+ 2.12\ X_1- 1.87\ X_2- 3.59\ X_3- 1.3\ X_1 X_2- 0.79\ X_1 X_3+ 0.3\ X_2 X_3- 2.89\ X_1^2- 0.468\ X_2^2+ 4.82\ X_3^2 \quad (3)$$

A positive zeta potential value was observed in all formulations due to the positive charge of chitosan [8]. Figure 1-e, f presented the response surface plot and cubic design for zeta potential response. Unlike the other two equations, it was seen that the effect of independent variables on zeta potential was best explained by the quadratic model. ANOVA results of this quadratic model for zeta potential were given in Table 1. It was observed that the greatest effect on zeta potential was the ultrasonicator amplitude. However, the R^2 value in this model remained at 0.7857, showing lower accuracy than the models created for particle size and PDI. Additionally, since $p>0.05$, the model could not be considered significant. Further, F-value of 2.85 implied there was a 9.05% chance that a Model F-value of this magnitude could occur due to noise.

Table 1. ANOVA results of the models for all responses

Source	Sum of squares	df	Mean square	F value	*p* value	R^2
Particle size (Y_1)						0.9992
Model	1044227.0	12	87018.9	424.58	<0.0001	
A	319937.3	1	319937.3	1561.03	<0.0001	
B	46203.5	1	46203.5	225.43	0.0001	
C	140010.7	1	140010.7	683.14	<0.0001	
AB	633.4	1	633.4	3.09	0.1536	
AC	122689.1	1	122689.1	598.62	<0.0001	
BC	67106.9	1	67106.9	327.43	<0.0001	
A^2	11744.6	1	11744.6	57.30	0.0016	
B^2	14861.7	1	14861.7	72.51	0.0010	
C^2	115519.0	1	115519.0	563.64	<0.0001	
A^2B	19863.5	1	19863.5	96.92	0.0006	
A^2C	1396.6	1	1396.6	6.81	0.0594	
AB^2	84240.1	1	84240.1	411.02	<0.0001	
Polidispersity index (Y_2)						0.9955
Model	0.444	12	0.037	73.59	0.0004	
A	0.163	1	0.163	324.99	<0.0001	
B	0.104	1	0.104	207.73	0.0001	
C	0.012	1	0.012	24.53	0.0077	
AB	0.008	1	0.008	15.48	0.0170	
AC	0.003	1	0.003	6.70	0.0608	
BC	0.00004	1	0.00004	0.07	0.8021	
A^2	0.017	1	0.017	34.30	0.0042	
B^2	0.009	1	0.009	17.71	0.0136	
C^2	0.074	1	0.074	148.95	0.0003	
A^2B	0.048	1	0.048	96.19	0.0006	
A^2C	0.007	1	0.007	13.17	0.0222	
AB^2	0.055	1	0.055	109.41	0.0005	
Zeta potential (Y_3)						0.7857
Model	304.60	9	33.84	2.85	0.0905	
A	35.98	1	35.98	3.03	0.1252	
B	28.10	1	28.10	2.37	0.1678	
C	102.96	1	102.96	8.67	0.0216	
AB	6.76	1	6.76	0.57	0.4751	
AC	2.50	1	2.50	0.21	0.6604	
BC	0.36	1	0.36	0.03	0.8667	
A^2	35.23	1	35.23	2.97	0.1286	
B^2	0.92	1	0.92	0.08	0.7887	
C^2	97.99	1	97.99	8.25	0.0239	

A: Chitosan:tripolyphosphate ratio (X_1), B: pH of chitosan solution (X_2), C: Ultrasonic homogenizer amplitude (X_3), df: Degrees of freedom

2.2. Validation of the models and the equations

As described in the method section, the model was validated by comparing measured and predicted responses and calculation of PE% (Table 2). In the models developed for particle size and PDI, the error was consistently below 15% across all formulations. A fairly uniform distribution was also obtained in the graph comparing predicted and actual values for particle size and PDI, respectively, from Figure 2-a and b.

Journal of Research in Pharmacy
Research Article

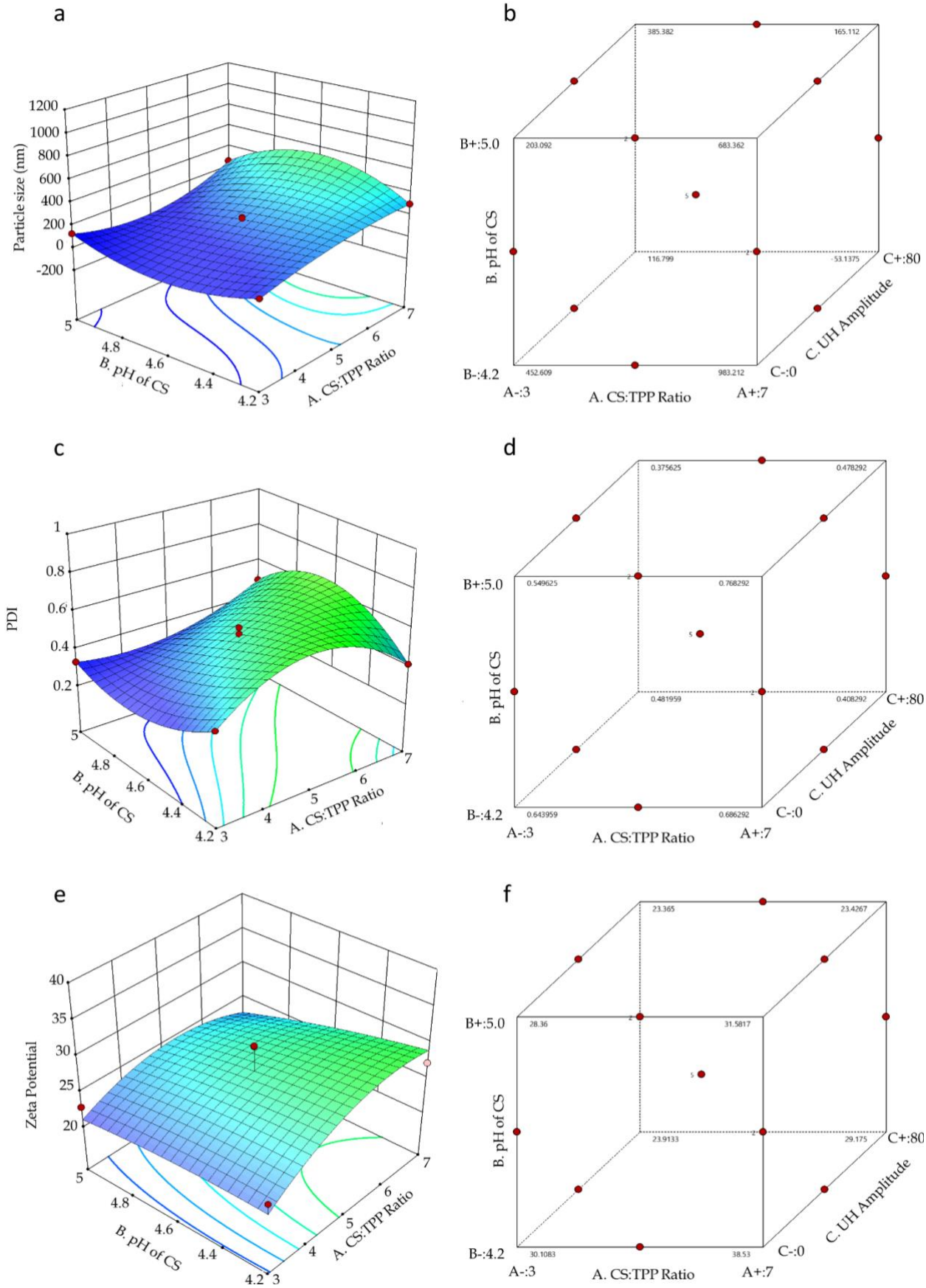

Figure 1. Response surface plots showing the effect of independent variables on a) particle size, c) PDI, e) zeta potential; and cube designs presenting the BBD model for responses: b) particle size, d) PDI, and f) zeta potential.

Moreover, the equations within these models demonstrated high accuracy, as evidenced by the robust R^2 values and statistical significance with *p* values less than 0.05, as previously discussed. This reaffirmed the validation of these two models, emphasizing their precision and reliability in yielding accurate results. In addition, in the 4th formulation of the model developed for zeta potential, the error was above 15%, which was the acceptable limit. Besides, compared to the models generated for particle size and PDI, higher error% values were obtained in the predicted zeta potential values of formulations. This situation was clearly seen in the predicted/actual data graph created for zeta potential in Figure 2-c. The fact that the model generated for zeta potential was not significant due to the *p* value and the R^2 value was lower than of the other models supports this situation.

Table 2. Experimental and theoretical values of the responses

Run	Particle size (nm)			PDI			Zeta potential (mV)		
	Actual	Predicted	Error %	Actual	Predicted	Error %	Actual	Predicted	Error %
1	182.03	182.02	0.005	0.477	0.477	0.000	29.70	29.70	0.000
2	205.37	208.01	1.285	0.561	0.526	6.237	30.50	27.09	11.180
3	320.63	320.62	0.003	0.655	0.655	0.000	26.77	26.76	0.037
4	105.27	105.26	0.009	0.309	0.309	0.000	20.90	24.10	15.311
5	299.4	301.4	0.668	0.414	0.414	0.000	27.23	29.02	6.570
6	149.2	149.2	0.000	0.393	0.393	0.000	27.70	26.28	5.117
7	258.6	260.6	0.773	0.490	0.490	0.000	21.27	22.68	6.657
8	226.57	208.01	8.192	0.512	0.526	2.676	30.63	27.09	11.567
9	218.6	208.01	4.844	0.501	0.526	4.860	25.60	27.09	5.820
10	193.1	208.01	7.721	0.527	0.526	0.184	23.90	27.09	13.347
11	738.33	738.34	0.001	0.827	0.827	0.000	35.80	37.20	3.918
12	264.33	264.32	0.004	0.510	0.510	0.000	31.07	32.86	5.769
13	1097.93	1097.94	0.001	0.939	0.939	0.000	38.73	35.52	8.288
14	105.1	105.1	0.000	0.722	0.722	0.000	31.23	29.42	5.788
15	119.07	117.06	1.688	0.430	0.430	0.016	23.60	22.18	6.006
16	128.6	126.58	1.571	0.329	0.329	0.040	22.83	21.04	7.843
17	196.43	208.01	5.895	0.528	0.526	0.373	24.83	27.09	9.087

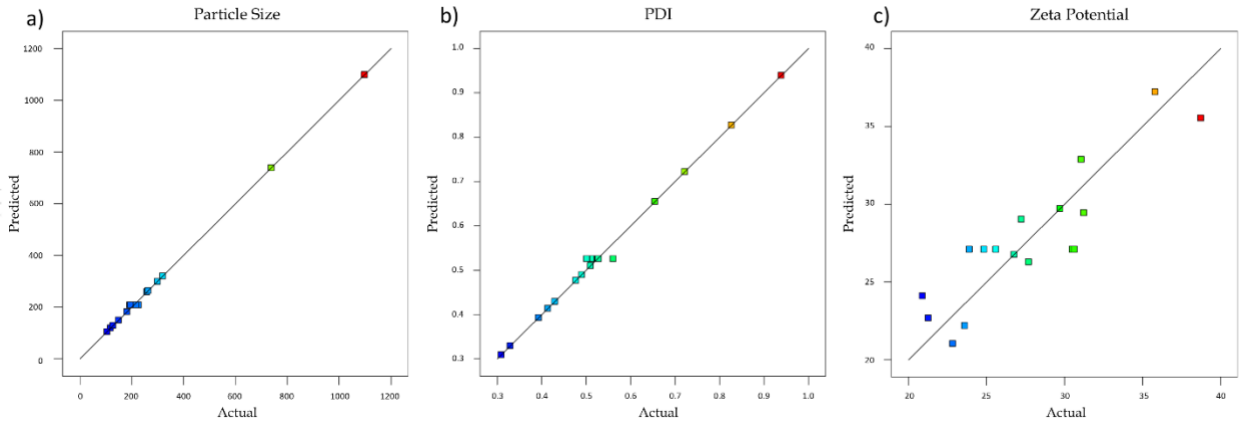

Figure 2. Curvature adjusted scatter plots of predicted data versus actual data of a) particle size, b) PDI, c) zeta potential

2.3. Physical stability of dispersed nanoparticles

The measurements were taken at two time points: initially (t = 0) and after one month of storage in a stability cabinet under conditions of 5°C ± 3°C, 25°C ± 2°C/60% ± 5% RH, or 40°C ± 2°C/75% ± 5% RH. The

changes in particle size, PDI, and zeta potential in the aqueous dispersions of formulations F1-18 (see Table 5) which were prepared after BBD optimization were shown in Figure 3.

The findings indicated significant variations in particle size across different formulations under diverse temperature and humidity conditions (see Figure 3-a, b, and c). The size distribution also changed over the time (Figure 3-d, e, and f). It was observed that particle size might either increase or decrease with rising temperature and relative humidity values. In chitosan-structured nanoparticles, the particle size could decrease due to chitosan degradation or increase due to swelling. Importantly, it should be noted that these swelling and degradation processes might occur concurrently. Lopez-Leon et al. conducted a similar study by storing dispersions of chitosan nanoparticles at different temperatures and found that the conformational change affected the particle size and also polydispersity due to the corrosion of chitosan nanoparticles in the aqueous environment and loss of their spherical shape [22].

Zeta potential changes in the formulations created less significant differences compared to particle size and PDI. Nevertheless, particularly under conditions of 40°C temperature and 75% relative humidity, a reduction in zeta potential values was observed in the dispersions, with some instances showing significant changes (Figure 3-g, h, and i). According to the DLVO theory, system stability is achieved when electrostatic repulsion dominates over attractive van der Waals forces [23]. For particles to aggregate, electrostatic repulsion must overcome the energy barrier. Particles with sufficient speed or kinetic energy collide, and elevated temperatures can intensify the kinetic energy, leading to particle aggregation and a decrease in zeta potential [24]. The observed decrease in zeta potential values may be attributed to this condition.

As a result, particle size, polydispersity, and zeta potential vary in aqueous dispersions of particles over time. This implies that chitosan–TPP nanogels behave as a metastable system and, therefore, they should be stored in a lyophilized state. Fresh aqueous solutions should only be prepared when needed.

3. CONCLUSION

In this study, the optimization of chitosan nanoparticles was pursued using the Box-Behnken Design. The chosen CPPs included the CS:TPP ratio, pH of the CS solution, and ultrasonic homogenizer amplitude, while the dependent variables comprised particle size, PDI, and zeta potential values. Individual models were constructed for each dependent variable through DoE, and the model accuracy was statistically assessed by ANOVA analysis and also comparing actual values with predicted values. Following these evaluations, it was observed that the particle size and polydispersity equations exhibited high accuracy (R^2= 0.9992 and R^2=0.9955, respectively). In addition, all error% values between the estimated and actual values for these particle size and PDI were within acceptable limits. However, the model for zeta potential did not yield significant results and higher unacceptable error values had obtained. Furthermore, alterations in these dependent variables were observed in the aqueous dispersions of nanoparticles stored under specific temperature and humidity conditions. This reiterates the necessity to lyophilize and store nanoparticles in a dry form.

4. MATERIALS AND METHODS

4.1. Materials

Chitosan with low molecular weight, sodium tripolyphosphate (TPP), and acetic acid were obtained from Sigma Aldrich, USA. Sodium hydroxide (NaOH) is purchased from Merck, Germany. All other reagents and solvents were of analytical grade. Design Expert 13 (Stat-Ease, USA) software was used for the DoE analysis.

4.2. Preparation of chitosan nanoparticles

CS was provided to form nanoparticles with TPP anions by the ionic gelation method. In this process, varying quantities of low molecular weight chitosan were dissolved in 1% (w/v) acetic acid solution and filtered through a 0.45 µm filter. Additionally, for each CS solution at different concentrations, the pH was ad-

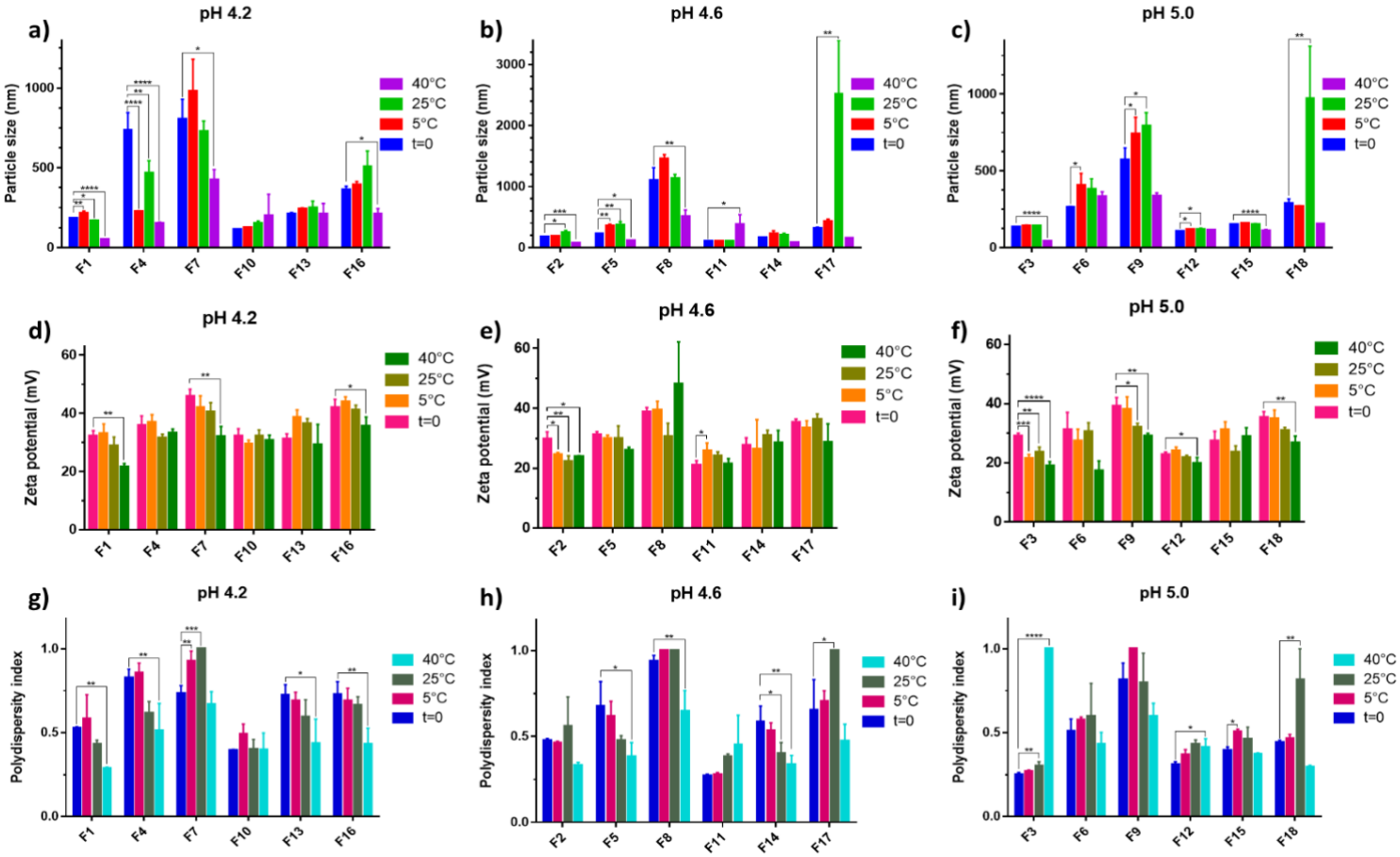

Figure 3. Change of responses after 30-day incubation of nanoparticle dispersions in stability cabinet at 5°C, 25°C/60% RH or 40°C/75%RH conditions for: Particle size of formulations prepared by using chitosan pH at a) 4.2, b) 4.6, and c) 5.0; zeta potential of formulations prepared by using chitosan pH at d) 4.2, e) 4.6, and f) 5.0; polydispersity index (PDI) of formulations prepared by using chitosan pH at g) 4.2, h) 4.6, and i) 5.0. All results were given as mean of n=3 and compared to responses at t=0 point. *$p<0.05$, **$p<0.01$, ***$p<0.001$, *and* ****$p<0.0001$

http://dx.doi.org/10.29228/jrp.788
J Res Pharm 2024; 28(4): 1057-1068

justed to different values using 0.1 M NaOH solution. 1 mg/mL concentration of TPP solution was also filtered through 0.45 µm filter following preparation with distilled water. To form the nanoparticles, 10 ml of the prepared chitosan solution was subjected to magnetic stirring, and concurrently, 10 ml of the TPP solution was added dropwise at a constant rate of 1.2 ml/min. In order to evaluate the effect of ultrasonic homogenizer (UH) on the formulation, ultrasonication was applied with either 40% or %80 amplitude, 20 kHz in an ice bath for 15 minutes during the addition of TPP solution in some of the formulations. In order to stabilize the dispersion, the particles were formed by mixing at 600 rpm with a magnetic stirrer at room temperature for 1 hour. All freeze-dried nanoparticles were stored at -20 °C for further studies.

4.3. Box-Behnken experimental design

In the present study, a Box-Behnken design with 3 factors and 3 levels was employed to formulate polynomial models for the optimization process. These levels of independent variables were illustrated in Table 3. BBD's rationale was predicated on its efficiency, which required 17 runs for this study according to equation 4:

$$N=2K(K-1)+C_{0,} \quad (4)$$

where N is the number of experiment, K is the number of factors and C_0 is the number of center points [25]. Center points allowed estimating the percentage error of the sum of squares, and five central repeat points were used for this purpose. This design was well-suited for scrutinizing the quadratic and cubic response surface and formulating a second or third-order polynomial model. The experimental design served to define the primary effects, interaction effects, and quadratic or cubic effects stemming from the formulation ingredients by incorporating both replicated center points and strategically positioned midpoints of each edge within the multidimensional cube. Thereby, it plays a pivotal role in optimizing the overall formulation process [18].

The non-linear model generated can be expressed as follows:

$$Y=A+\sum_{i=1}^{3} B\,X_i+{}_1+\sum_{i,j=1}^{3} C\,X_iX_j+\sum_{i,j=1}^{3} D\,X_i^2X_j \quad (5)$$

Here, A is a constant term, B_i represents the coefficients associated with the linear terms, C_{ij} represents the coefficients associated with the quadratic interaction terms, and D_{ij} represents the coefficients associated with the cubic interaction terms. Additionally, Y signifies the measured response of dependent variables corresponding to each factor-level (X) combination. Independent variables were chosen as CS:TPP ratio (X_1), pH of CS solution (X_2) and UH amplitude% (X_3). The dependent variables investigated comprised particle size (Y_1), PDI (Y_2), and zeta potential (Y_3). ANOVA method was used to analyze the statistical significance of the established experimental model. Table 4 shows the experimental design matrix generated by the software.

$$Error\%=|(Calculated-measured)/measured|\,x\,100 \quad (6)$$

Table 3. List of variables in Box-Behnken design for the optimization of chitosan nanoparticles

	Levels		
	-1	**0**	**+1**
Factors			
X_1: CS:TPP ratio	3:1	5:1	7:1
X_2: pH of CS solution	4.2	4.6	5.0
X_3: UH amplitude %	0	40	80
Responses			
Y_1: Particle size (nm)			
Y_2: PDI			
Y_3: Zeta potential (mV)			

CS: Chitosan, TPP: Tripolyphosphate, UH: Ultrasonic homogenizer, PDI: Polydispersity index

4.4. Analysis of particle size, polidispersity and zeta potential

Particle size and size distribution was measured by dynamic light scattering method using Malvern NanoZS Zen 3600 (Malvern Instruments LTD., Malvern, UK). Nanoparticles were dispersed in distilled water, and the Z-average was used to determine the average particle size. Particle size distribution was assessed through the PDI values of the formulations. The zeta potential of the nanoparticles was also measured by NanoZS Zen 3600 and expressed as mean.

4.5. Validation of the model and the equations

A validation study was carried out to verify the accuracy of the created BBD and the obtained equations In this context, the measured (actual) values for particle size, PDI, and zeta potential were compared with the predicted values derived from the BBD equations for all formulations. Error% was then calculated using equation 6, and the predictions with error%<15% were considered acceptable [13, 26].

Table 4. 3-level Box-Behnken design

Run	CS:TPP Ratio (X_1)	pH of CS Solution (X_2)	UH Amplitude (%, X_3)
1	3	4.6	0
2	5	4.6	40
3	7	4.6	80
4	3	4.6	80
5	7	4.2	40
6	5	5	80
7	7	5	40
8	5	4.6	40
9	5	4.6	40
10	5	4.6	40
11	5	4.2	0
12	5	5	0
13	7	4.6	0
14	5	4.2	80
15	3	4.2	40
16	3	5	40
17	5	4.6	40

CS: Chitosan, TPP: Tripolyphosphate, UH: Ultrasonic homogenizer, PDI: Polydispersity index

4.6. Evaluation of physical stability of dispersed nanoparticles

This study was carried out to evaluate whether chitosan nanoparticles would maintain their physical stability after being dispersed. For this purpose, 18 formulations were prepared, the formulation parameters of which are given in Table 5. Then, the particle size, PDI and zeta potential in the aqueous dispersions of these nanoparticles were measured. Following the initial measurements, the aqueous dispersions of nanoparticles were kept in the stability cabinet at 5°C ± 3°C, 25°C ± 2°C/60% ± 5% RH, and 40°C ± 2°C/75% RH ± 5% RH conditions separately, taking into account the ICH Q2 guide. After 30 days, the formulations

were terminally evaluated in terms of particle size, particle size distribution, and zeta potential. The results were compared to the initial time point (t=0), and statistical analysis was conducted using the one-way ANOVA method with a 95% confidence interval. Thus, dispersion stability was assessed based on the observed changes relative to the initial measurements.

Table 5. Formulation parameters of final nanoparticle formulations

Formulation	CS:TPP Ratio	pH of CS Solution	UH Amplitude (%)
F1	3	4.2	0
F2	3	4.6	0
F3	3	5.0	0
F4	5	4.2	0
F5	5	4.6	0
F6	5	5.0	0
F7	7	4.2	0
F8	7	4.6	0
F9	7	5.0	0
F10	3	4.2	80
F11	3	4.6	80
F12	3	5.0	80
F13	5	4.2	80
F14	5	4.6	80
F15	5	5.0	80
F16	7	4.2	80
F17	7	4.6	80
F18	7	5.0	80

CS: Chitosan, TPP: Tripolyphosphate, UH: Ultrasonic homogenizer, PDI: Polydispersity index

Acknowledgements: The study is a part of PhD thesis in Institute of Health Sciences, Marmara University. This study is supported by Health Institutes of Türkiye (TÜSEB) with project number of 11933.

Author contributions: Concept – S.Ö.Ö., T.U..; Design – S.Ö.Ö..; Supervision – T.U.; Resources – S.Ö.Ö., T.U.; Materials – S.Ö.Ö., T.U.; Data Collection and/or Processing – S.Ö.Ö.; Analysis and/or Interpretation – S.Ö.Ö.; Literature Search – S.Ö.Ö. Writing – S.Ö.Ö..; Critical Reviews – T.U.

Conflict of interest statement: The authors declared no conflict of interest.

REFERENCES

[1] Bayda S, Adeel M, Tuccinardi T, Cordani M, Rizzolio F. The history of nanoscience and nanotechnology: From chemical-physical applications to nanomedicine. Molecules. 2019; 25(1): 112. https://doi.org/10.3390/molecules25010112

[2] Yusuf A, Almotairy ARZ, Henidi H, Alshehri OY, Aldughaim MS. Nanoparticles as drug delivery systems: A review of the implication of nanoparticles' physicochemical properties on responses in biological systems. Polymers (Basel). 2023 ;15(7): 1596. https://doi.org/10.3390/polym15071596

[3] Zielińska A, Carreiró F, Oliveira AM, Neves A, Pires B, Venkatesh DN, Durazzo A, Lucarini M, Eder P, Silva AM, Santini A, Souto EB. Polymeric nanoparticles: Production, characterization, toxicology and ecotoxicology. Molecules. 2020; 25(16): 3731. https://doi.org/10.3390/molecules25163731

[4] Dhanjal DS, Mehta M, Chopra C, Singh R, Sharma P, Chellappan DK, Tambuwala MM, Bakshi HA, Aljabali AAA, Gupta G, Nammi S, Prasher P, Dua K, Satija S. Chapter 15 - Novel Controlled Release Pulmonary Drug Delivery Systems: Current updates and Challenges. In: Azar AT (Ed). Modeling and Control of Drug Delivery Systems. Academic Press, 2021, pp. 253-272.

[5] Chandy T, Sharma CP. Chitosan-as a biomaterial. Biomater Artif Cells Artif Organs. 1990; 18(1): 1-24. https://doi.org/10.3109/10731199009117286

[6] Harugade A, Sherje AP, Pethe A. Chitosan: A review on properties, biological activities and recent progress in biomedical applications. React Funct Polym. 2023; 191: 105634. https://doi.org/10.1016/j.reactfunctpolym.2023.105634.

[7] Ways TMM, Lau WM, Khutoryanskiy VV. Chitosan and its derivatives for application in mucoadhesive drug delivery systems. Polymers (Basel). 2018; 10(3): 267. https://doi.org/10.3390/polym10030267.
[8] Chua BY, Al Kobaisi M, Zeng W, Mainwaring D, Jackson DC. Chitosan microparticles and nanoparticles as biocompatible delivery vehicles for peptide and protein-based immunocontraceptive vaccines. Mol Pharmaceutics. 2012; 9(1): 81-90. https://doi.org/10.1021/mp200264m
[9] Yang X, Yuan X, Cai D, Wang S, Zong L. Low molecular weight chitosan in DNA vaccine delivery via mucosa. Int J Pharm. 2009; 375(1-2): 123-32. https://doi.org/10.1016/j.ijpharm.2009.03.032
[10] Fei Liu X, Lin Guan Y, Zhi Yang D, Li Z, De Yao K. Antibacterial action of chitosan and carboxymethylated chitosan. J Appl Poly Sci. 2001; 79(7): 1324-1335. https://doi.org/10.1002/1097-4628(20010214)79:7<1324::AID-APP210>3.0.CO;2-L
[11] Sawaengsak C, Mori Y, Yamanishi K, Mitrevej A, Sinchaipanid N. Chitosan nanoparticle encapsulated hemagglutinin-split influenza virus mucosal vaccine. AAPS PharmSciTech. 2014; 15: 317-325. https://doi.org/10.1208/s12249-013-0058-7
[12] Svindland SC, Pedersen GK, Pathirana RD, Bredholt G, Nøstbakken JK, Jul-Larsen Å, Guzmán CA, Montomoli E, Lapini G, Piccirella S, Jabbal-Gill I, Hinchcliffe M, Cox RJ. A study of Chitosan and c-di-GMP as mucosal adjuvants for intranasal influenza H5N1 vaccine. Influenza Other Respir Viruses. 2013; 7(6): 1181-1193. https://doi.org/10.1111/irv.12056
[13] Mahmoud BS, McConville C. Box-Behnken design of experiments of polycaprolactone nanoparticles loaded with irinotecan hydrochloride. Pharmaceutics. 2023; 15(4): 1271. https://doi.org/ 10.3390/pharmaceutics15041271
[14] Antony J. Design of experiments for engineers and scientists, third ed., Elsevier, USA 2023. https://doi.org/10.1016/C2022-0-01075-8
[15] Ghanbarzadeh S, Khorrami A, Arami S. Preparation of optimized naproxen nano liposomes using response surface methodology. J Pharm Investig. 2014; 44: 33-39. https://doi.org/10.1007/s40005-013-0098-8
[16] Guterres SS, Weiss V, De Lucca Freitas L, Pohlmann AR. Influence of benzyl benzoate as oil core on the physicochemical properties of spray-dried powders from polymeric nanocapsules containing indomethacin. Drug Deliv. 2000; 7(4): 195-199. https://doi.org/ 10.1080/107175400455119
[17] Thompson D. Response surface experimentation 1. J Food Process Preserv. 1982; 6(3): 155-188. https://doi.org/10.1111/j.1745-4549.1982.tb00650.x
[18] Hao J, Fang X, Zhou Y, Wang J, Guo F, Li F, Peng X. Development and optimization of solid lipid nanoparticle formulation for ophthalmic delivery of chloramphenicol using a Box-Behnken design. Int J Nanomed. 2011; 6: 683-692. https://doi.org/10.2147/ijn.S17386
[19] Abyadeh M, Karimi Zarchi AA, Faramarzi MA, Amani A. Evaluation of factors affecting size and size distribution of chitosan-electrosprayed nanoparticles. Avicenna J Med Biotechnol. 2017; 9(3): 126-132.
[20] Masarudin MJ, Cutts SM, Evison BJ, Phillips DR, Pigram PJ. Factors determining the stability, size distribution, and cellular accumulation of small, monodisperse chitosan nanoparticles as candidate vectors for anticancer drug delivery: application to the passive encapsulation of [(14)C]-doxorubicin. Nanotechnol Sci Appl. 2015; 8: 67-80. https://doi.org/10.2147/nsa.S91785
[21] Wu L, Zhang J, Watanabe W. Physical and chemical stability of drug nanoparticles. Adv Drug Deliv Rev. 2011; 63(6): 456-469. https://doi.org/10.1016/j.addr.2011.02.001.
[22] López-León T, Carvalho ELS, Seijo B, Ortega-Vinuesa JL, Bastos-González D. Physicochemical characterization of chitosan nanoparticles: electrokinetic and stability behavior. J Colloid Interface Sci. 2005; 283(2): 344-351. https://doi.org/10.1016/j.jcis.2004.08.186.
[23] Lagaly G. Energetische wechselwirkungen in dispersionen und emulsionen. In: Technologie von Salben, Suspensionen und Emulsionen. Wissenschaftliche Verlagsgesellschaft, Stuttgart, Germany, 1984, pp. 32-61.
[24] Freitas C, Müller RH. Effect of light and temperature on zeta potential and physical stability in solid lipid nanoparticle (SLN™) dispersions. Int J of Pharm. 1998; 168(2): 221-229. https://doi.org/10.1016/S0378-5173(98)00092-1
[25] Salari M. Optimization by Box–Behnken Design and Synthesis of Magnetite Nanoparticles for Removal of the Antibiotic from an Aqueous Phase. Adsorp Sci Technol. 2022; 2022: 1267460. https://doi.org/10.1155/2022/1267460
[26] Maleki Dizaj S, Lotfipour F, Barzegar-Jalali M, Zarrintan M-H, Adibkia K. Box-Behnken experimental design for preparation and optimization of ciprofloxacin hydrochloride-loaded CaCO3 nanoparticles. J Drug Deliv Sci Technol. 2015; 29: 125-131. https://doi.org/10.1016/j.jddst.2015.06.015